10-1-2001

Photochemical Escape of Atomic Carbon from Mars

Jane L. Fox
Wright State University - Main Campus, jane.fox@wright.edu

F. M. Bakalian

JOURNAL OF GEOPHYSICAL RESEARCH, VOL. 106, NO. A12, PAGES 28,785–28,795, DECEMBER 1, 2001

Photochemical escape of atomic carbon from Mars

J. L. Fox[1] and F. M. Bakalian
Institute for Terrestrial and Planetary Atmospheres, State University of New York at Stony Brook, New York, USA

Abstract. We have modeled the escape fluxes of atomic carbon from the Martian atmosphere for low and high solar activities due to various photochemical escape mechanisms, including photodissociation of CO, dissociative recombination of CO^+, electron impact dissociation and dissociative ionization of CO, photodissociative ionization of CO, and dissociative charge transfer of O^{++} to CO. Only photodissociation of CO and dissociative recombination of CO^+ are found to be important, and the time-averaged escape flux is predicted to be controlled by the high solar activity values. The computed global average escape fluxes of C due to photodissociation of CO at low and high solar activities are 1.65×10^5 and 1.8×10^6 cm^{-2} s^{-1}, respectively, and those for dissociative recombination are 2.9×10^4 and 6.2×10^5 cm^{-2} s^{-1}, respectively. The other sources contribute <10% to the total. The photochemical escape rates are slightly larger than those estimated for sputtering by O^+ pickup ions in the present era. If current estimates are correct, however, sputtering will dominate the escape in earlier epochs when the solar wind is predicted to have been much stronger. Ion outflow may also constitute an important loss mechanism if escape rates are on the order of their predicted upper limits.

1. Introduction

Geological evidence suggests that the early atmosphere of Mars was thicker, warmer, and wetter than it is at present, and the observed enrichment in heavy isotopes indicates that escape to space plays an important role in the loss of volatiles [e.g., *Jakosky*, 1991; *Jakosky and Jones*, 1997]. Nonthermal mechanisms by which heavy species, such as C, N, and O, may escape from the atmosphere of Mars have been identified but not completely quantified. The production of energetic atoms also results in the formation of hot atom coronas in which atoms that do not have enough energy to escape may travel to great heights along ballistic trajectories before falling again because of the gravitational attraction of the planet.

Knowledge of the escape processes for C and O, in particular, is crucial to reconstructing the time-dependent Martian inventory of CO_2. Estimated values for the current O escape fluxes due to dissociative recombination and/or sputtering by O^+ pickup ions cover a very wide range of 3×10^6 to 1.4×10^8 cm^{-2} s^{-1} [*Lammer and Bauer*, 1991; *Fox*, 1993; *Zhang et al.*, 1993; *Luhmann*, 1997; *Kass and Yung*, 1995, 1996; *Johnson and Liu*, 1996; *Lammer et al.*, 1996; *Kass*, 1999; *Kim et al.*, 1998; *Johnson et al.*, 2000; *Hodges*, 2000]. In addition, some loss of O as O^+ or O_2^+ ions is predicted, and large fluxes of escaping ions have been measured by instruments on the Phobos spacecraft [e.g., *Verigin et al.*, 1991; *Lundin et al.*, 1990]. *Zhang et al.* [1993] estimated a fairly low escape flux of 8×10^6 cm^{-2} s^{-1} for solar wind pickup of O^+ ions produced by ionization of O above the ionopause. *Fox* [1997], however, pointed out that potentially all the ions produced above the photochemical equilibrium region could be lost by outward flow and computed upper limits to the hemispheric escape fluxes of O_2^+ and O^+ of 4.7×10^7 and 6.7×10^6 cm^{-2} s^{-1}, respectively, for low solar activity, and 1.35×10^8 and 1.8×10^7 cm^{-2} s^{-1}, respectively, for high solar activity. High solar activity MHD calculations by *Liu et al.* [1999, 2001] predicted that the total hemispheric escape fluxes for $O_2^+ + O^+$ were of the order of 3.8×10^7 cm^{-2} s^{-1} out of a total of $\sim 7.7 \times 10^7$ ions cm^{-2} s^{-1} crossing the terminator plane. These values are about one fourth and one half of our upper limits of $(5\text{–}15) \times 10^7$ cm^{-2} s^{-1} where the range is from low to high solar activity. Our predicted upper limit to the hemispheric average escape flux of O in all ions is $(1.1\text{–}3.5) \times 10^8$ cm^{-2} s^{-1} where the range is for low to high solar activities, and thus the upper limit to the global average escape flux, which is half the hemispheric value, is $\sim 1.2 \times 10^8$ cm^{-2} s^{-1}. Although there is significant disagreement about the total escape rate of oxygen, the predicted O escape rates at the current epoch are much

[1]Also at Department of Physics, Wright State University, Dayton, Ohio

Paper number 2001JA000108.
0148-0227/01/2001JA000108$09.00

larger than estimates of the atomic carbon escape rates, and therefore loss to space of CO_2 from Mars can be assumed to be controlled by the escape rate of C.

A number of photochemical escape mechanisms have been identified that may produce C atoms with energies in excess of the escape energy, which is ~ 1.48 eV at the Martian exobase. *McElroy* [1972] (see also *McElroy et al.* [1977]) and *Wallis* [1989] enumerated some of the possible processes, which include dissociative recombination of CO^+,

$$CO^+ + e \rightarrow C + O, \quad (1)$$

photoelectron impact dissociation of CO,

$$CO + e^* \rightarrow C + O + e \quad (2)$$

and photodissociation of CO,

$$CO + h\nu \rightarrow C + O. \quad (3)$$

Other potential sources of escaping C atoms include photodissociative ionization of CO,

$$CO + h\nu \rightarrow C + O^+ + e \quad (4)$$

and photoelectron impact dissociative ionization,

$$CO + e^* \rightarrow C + O^+ + 2e, \quad (5)$$

as such processes have been found to produce highly translationally excited fragments. For example, *Mathur and Eland* [1992] carried out coincidence time-of-flight mass spectrometry for photodissociative ionization of CO at several discrete photon energies between 22.5 and 48.5 eV and found that the fragments produced possessed kinetic energies of up to several eV. Electron impact dissociative ionization of the isoelectronic molecule N_2 has also been shown to produce very energetic atoms and ions [*Morgan and Mentall*, 1983]. The dissociative charge transfer reaction of O^{++} with CO,

$$O^{++} + CO \rightarrow C + O^+ + O^+, \quad (6)$$

is exothermic by 10.4 eV if all the products are in their ground states, and the reaction will probably produce C atoms with energies in excess of the escape energy. Dissociative recombination of CO_2^+ and electron impact dissociation of CO_2 have also been suggested as sources of hot and escaping C, but there is little information on the production of C in these processes, and the major products are probably CO and O.

We estimate here, for both high and low solar activities, the production rate of hot and escaping C from the most important nonthermal sources. We have evaluated dissociative recombination as a source of hot C previously using somewhat different models [*Fox and Haćić*, 1999]. We estimate the magnitudes of the photochemical sources (reactions (1)–(6)) of energetic C, using revised models for the thermospheres/ionospheres of Mars at high and low solar activities. Photodissociation has been shown to be the most important source of thermal C on Venus [*Krasnopolsky*, 1982; *Fox*, 1982; *Fox and Sung*, 2001]. Photodissociation of CO proceeds via line absorption into predissociating states between the threshold at 1118 Å and 889 Å and by continuum absorption shortward of 889 Å. *Fox and Black* [1989] constructed high-resolution cross sections in this wavelength region and demonstrated that the photodissociation rate of CO is smaller by a factor of ~ 2 at the low temperatures appropriate to the Venus and Mars thermospheres than previous models using the low-resolution cross sections had indicated [e.g., *Fox*, 1982; *Krasnopolsky*, 1982]. The effect of the use of these higher-resolution cross sections on the escape fluxes is limited because photons with wavelengths longward of 905 Å cannot produce escaping C atoms. We adopt here the cross sections constructed by *Fox and Black* [1989], averaged over 1 Å intervals for absorption in the 889 to 1118 Å region, and those of *Samson and Gardner* [1976] at wavelengths shortward of 889 Å. Preliminary calculations for a moderate solar activity model [*Fox*, 1999] and for a high solar activity model [*Fox*, 2000] showed that the escape flux due to photodissociation of CO was more important than, but comparable to, that due to dissociative recombination of CO^+.

Nagy et al. [2001] have recently used a two-stream method with the production rates from our previous models to investigate the hot C corona of Mars. We provide here a more detailed explanation of some of the assumptions used in those calculations. They found, as we have, that photodissociation of CO and dissociative recombination of CO^+ were the most important sources. *Paxton* [1983] demonstrated that collisions of hot O atoms with thermal C were a major source of the hot C corona at Venus and more important than dissociative recombination of CO^+. *Nagy et al.* [2001] have shown, however, that this source is negligible at Mars, either for production of the hot C corona or for escape of atomic carbon. *Paxton* [1983] did not consider photodissociation of CO as a source of hot C on Venus.

We compare our estimated escape fluxes using the "exobase approximation" with those obtained by *Nagy et al.* [2001] for photodissociation of CO and dissociative recombination of CO^+ using the two-stream approach and with those estimated for the current atmosphere due to sputtering of C by O^+ pickup ions by *Luhmann et al.* [1992] (as corrected by *Jakosky et al.* [1994]) and by *Kass* [1999].

2. Model

We have constructed a model of the high solar activity thermosphere and ionosphere from neutral density profiles of CO_2, N_2, O, CO, and O_2 derived from the Mars thermospheric general circulation model (MTGCM) for 2.5° latitude and 1600 LT, supplied to us by S. W. Bougher (private communication, 1999) [see also *Bougher et al.*, 1990]. The low solar activity model is based on the Viking measurements of CO_2, N_2, Ar,

CO, O_2, and NO, for which the solar zenith angle was 44°. The eddy diffusion coefficients were adjusted to match the N_2 profiles in both models and then used to compute the density profiles of other species. The Ar mixing ratio at the bottom boundary of the high solar activity model was assumed to be the same as that derived from the Viking data, 0.015 [e.g., *Nier and McElroy*, 1976, 1977]. Since we do not include the chemistry of odd hydrogen in the middle atmosphere, the H density profiles were obtained by adjusting the density at the bottom boundary, 80 km, so that the high-altitude values matched those inferred from measurements of the Lyman alpha airglow. Consequently, the atomic hydrogen densities near the lower boundary are somewhat arbitrary and should not be considered as reliable as those computed for the middle and upper atmosphere by, for example, *Krasnopolsky* [1993a, 1993b] or *Nair et al.* [1994]. The H density at 250 km at high solar activity was assumed to be $3 \times 10^4\,cm^{-3}$, close to that derived from the Mariner 6 and 7 Lyman alpha measurements [*Barth et al.*, 1971; *Anderson and Hord*, 1971]. For the low solar activity model the H density at 250 km was adjusted to approximate the value of $\sim 1.4 \times 10^6\,cm^{-3}$ derived from the recent Hubble Space Telescope measurements of *Krasnopolsky et al.* [1998] [see also *Krasnopolsky*, 2000]. The mixing ratio of He was assumed to be 4 ppm at the bottom boundary [*Krasnopolsky and Gladstone*, 1996]. The H_2 mixing ratio at the bottom boundaries of both models was taken to be 40 ppm, as suggested by the model calculations presented by *Krasnopolsky et al.* [1998]. The neutral density profiles for the low and high solar activity models are shown in Figures 1a and 1b. In these figures the density profiles that were adopted from Viking measurements or the MTGCM are shown as solid curves, while the N, NO, and C densities, which were computed self-consistently in the models, are shown as dashed curves. The density profiles of the light species H, H_2, and He, which were calculated as described above, are represented by dotted curves.

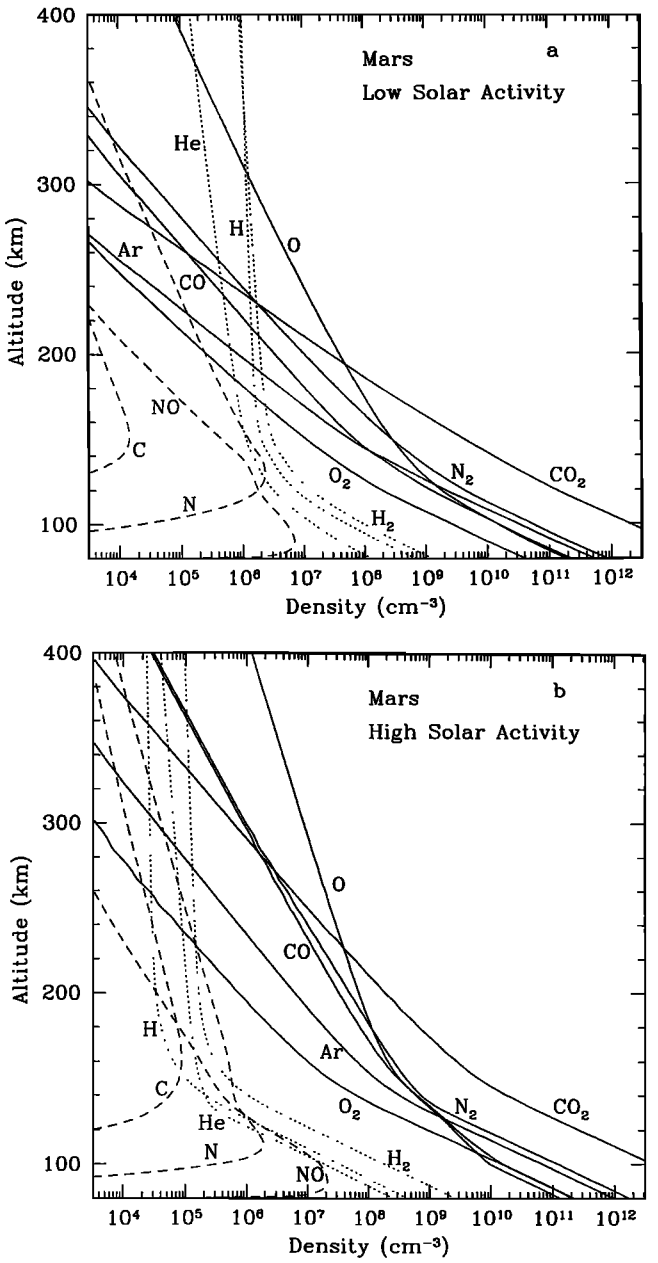

Figure 1. (a) Density profiles of the neutral species for the low solar activity Mars thermosphere. The model is based largely on the measured densities of Viking 1 [e.g., *Nier and McElroy*, 1977]. (b) Density profiles of the most important neutral species for the high solar activity Mars thermosphere. This model is based largely on the Mars thermospheric general circulation model of S. Bougher (private communication, 1999).

In order to estimate the escape rates it is necessary to locate the exobases in both models. *Tully and Johnson* [2001] have discussed this issue in conjunction with their ab initio calculations of the O–O elastic and momentum transfer cross sections (σ_d). They assert that the exobase should be placed at a column density of $\sim 1.3/\sigma_d$. Unfortunately, there is little information about elastic or momentum transfer cross sections for collisions of C with any atmospheric gases. The major constituents of the Martian exosphere are CO_2 and O, although the H and H_2 column densities are significant at low solar activity. *Kharchenko et al.* [2000] computed the elastic cross sections for O–O collisions and reported values decreasing smoothly from $\sim 7 \times 10^{-15}$ cm^2 at 1 eV to 5.5×10^{-15} cm^2 at 5 eV. *Tully and Johnson* [2001] carried out similar calculations for different potential surfaces and obtained elastic cross sections that decreased with energy from $2.5 \times 10^{-15}\,cm^2$ at 1 eV to $2 \times 10^{-15}\,cm^2$ at 5 eV and momentum transfer cross sections that decreased from $\sim 1.5 \times 10^{-15}$ cm^2 to about half that value over the same energy range. *Kharchenko et al.* [1997] computed the elastic and momentum transfer cross sections for O–N scattering and found that the former decreased from 10×10^{-15} to $8 \times 10^{-15}\,cm^2$, and the latter from 1.3×10^{-15} to 1.1×10^{-15} cm^2 over the energy range 1–5 eV. *Balakrishnan et al.* [1998] carried out calculations of the elastic cross sections for N +

N_2 collisions and reported values near 7×10^{-15} cm^2 in the energy range for relative motion of 1–3 eV. In general, where they are available, the computed momentum transfer cross sections are smaller than the elastic cross sections by factors of 2 or more. We have assumed here an average momentum transfer cross section of 3×10^{-15} cm^2 for near escape velocity collisions of C atoms with exospheric species, which places the exobase at $\sim$ 188 km for the low solar activity model and at $\sim$220 km for the high solar activity model.

We have adopted the solar fluxes from the high solar activity F79050N spectrum of H. E. Hinteregger (private communication, 1981) [see also *Torr et al.*, 1979], in which photon fluxes from 18 to 2000 Å are given in the continua at 1 Å resolution and as integrated fluxes at the strong solar lines. We have extended the solar spectrum to X rays shortward of 18 Å using the high solar activity model of *Ayres* [1997; also private communication, 1997], with solar fluxes given in 1 Å bins. In the low solar activity model, the Ayres X-ray fluxes were assumed, somewhat arbitrarily, to be smaller by a factor of 10. In order to approximate average dayside conditions the solar zenith angle is taken to be 60°.

Recently, evidence has been adduced that the Hinteregger solar fluxes in the soft X-ray region are too small by factors of 2–4 [e.g., *Bailey et al.*, 2000]. *Fox et al.* [1995] constructed high and low solar activity models of the Martian ionosphere/thermosphere using solar fluxes from *Tobiska* [1991], which also exhibited larger fluxes in the soft X-ray region, and compared them with models computed with the Hinteregger solar fluxes. The electron densities below 120 km were much larger when computed with the Tobiska fluxes than with the Hinteregger fluxes, but the topside profile showed little effect. Thus we expect that increasing the soft X-ray fluxes would have a large effect on the

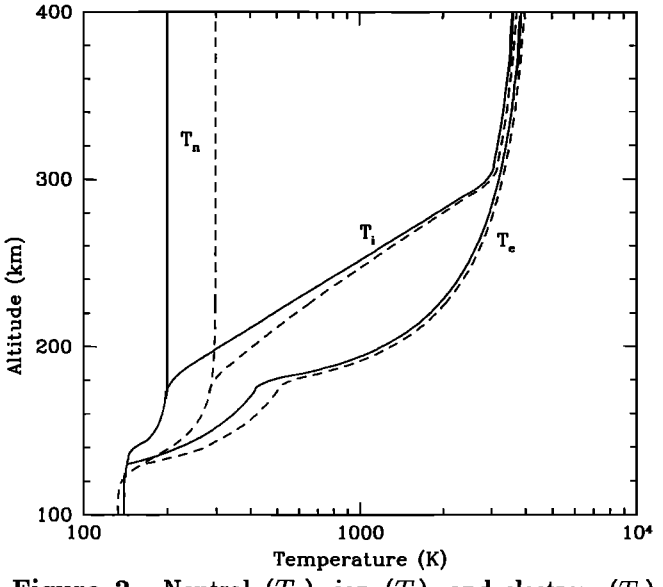

Figure 2. Neutral (T_n), ion (T_i), and electron (T_e) temperatures assumed in the models. The solid curves are the low solar activity values and the dashed curves are the high solar activity values. The low solar activity ion temperature profile is based on the Viking measurements [*Hanson et al.*, 1977], and the electron temperatures are based on the calculations of *Rohrbaugh et al.* [1979]. Since the Viking retarding potential analyzer did not measure the ion temperatures above 300 km, the profile above that altitude is uncertain. The high solar activity plasma temperatures are assumed, somewhat arbitrarily, to be larger than the low solar activity values by the difference between the high and low solar activity neutral temperatures.

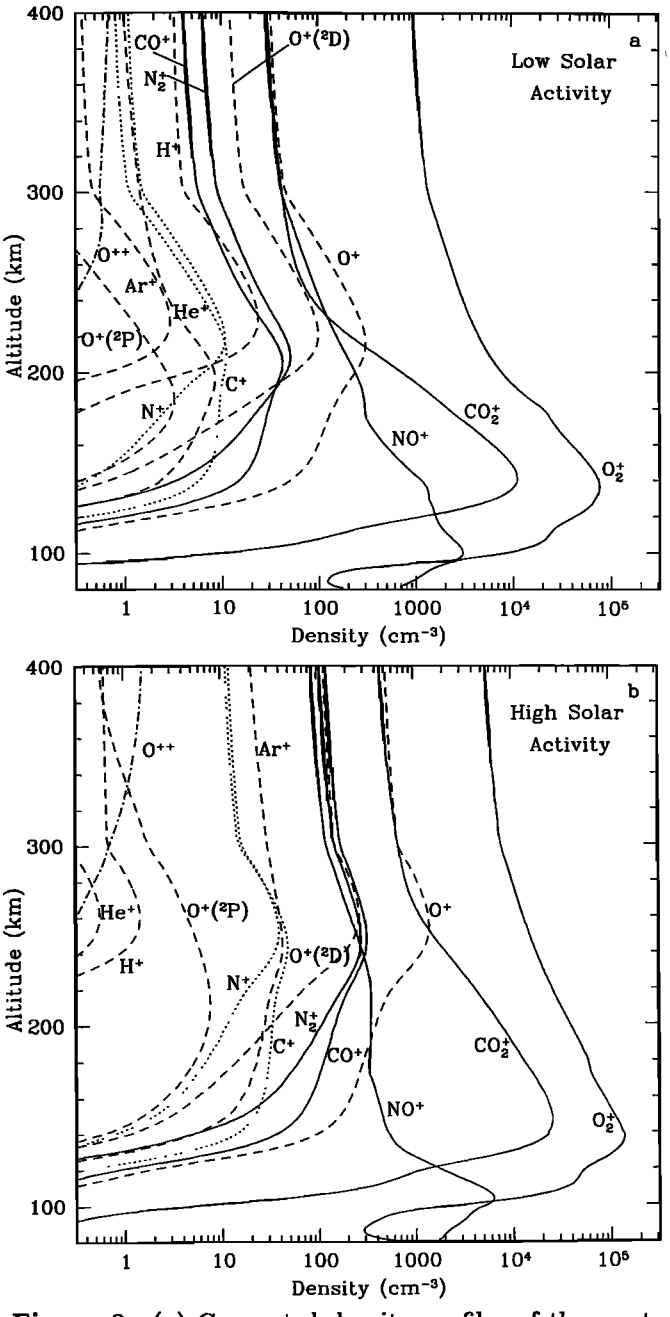

Figure 3. (a) Computed density profiles of the most important ions for the low solar activity model. (b) Computed density profiles of the most important ions for the high solar activity model.

ionosphere/thermosphere below the ionospheric peak but very little in the exobase region.

The chemical reaction scheme employed has been updated from that of our previous models [e.g., *Fox*, 1982, 1993], and a complete list of reactions and their rate coefficients is presented by *Fox and Sung* [2001]. The cross sections for photoabsorption, photoionization, and photodissociation are also similar to those which we have used previously, and the recent revisions are also listed by *Fox and Sung* [2001]. Our compilation of electron impact cross sections has been presented by *Sung and Fox* [2000] and will be submitted for publication soon (K. Y. Sung and J. L. Fox, manuscript in preparation, 2001). The ion and electron temperatures adopted are shown in Figure 2. The computed steady state ion density profiles for the current models are shown in Figures 3a and 3b.

3. Escape Mechanisms

The rate coefficient for dissociative recombination of CO^+ has been measured by a number of investigators with widely varying results. *Mentzoni and Donohoe* [1969] made the first measurement of the rate coefficient in a flowing afterglow experiment and reported a very large value near 300 K of $6.8 \times 10^{-7}\,cm^3\,s^{-1}$. Using a merged beam apparatus, *Mitchell and Hus* [1985] obtained a thermal rate coefficient of $2 \times 10^{-7}\,cm^3\,s^{-1}$, which was later revised downward to $1 \times 10^{-7}\,cm^3\,s^{-1}$ because of a factor of 2 error in the calibration of the beam [*Mitchell*, 1990]. Flowing afterglow–Langmuir probe–mass spectrometer experiments by *Geoghegan et al.* [1991] and more recently by *Laubé et al.* [1998] have yielded thermal rate coefficients of 1.6×10^{-7} and $1.85 \times 10^{-7}\,cm^3\,s^{-1}$, respectively. *Rosén et al.* [1998] recently employed a heavy-ion storage ring to measure the temperature dependent dissociative recombination coefficient; a value of $2.75 \times 10^{-7}\,cm^3\,s^{-1}$ was reported at 300 K.

The dissociative recombination of CO^+ may proceed by a number of channels, which are enumerated below along with their exothermicities:

$$CO^+ + e \rightarrow C(^3P) + O(^3P) + 2.90\,eV \quad (1a)$$

$$CO^+ + e \rightarrow C(^1D) + O(^3P) + 1.64\,eV \quad (1b)$$

$$CO^+ + e \rightarrow C(^3P) + O(^1D) + 0.94\,eV \quad (1c)$$

$$CO^+ + e \rightarrow C(^1S) + O(^3P) + 0.22\,eV \quad (1d)$$

$$CO^+ + e \rightarrow C(^1D) + O(^1D) - 0.33\,eV. \quad (1e)$$

Escape is possible for C atoms produced only in channel (1a). The branching ratios of channels (1a)–(1e) have been measured by *Rosén et al.* [1998] at 0 and 0.4 eV relative energy. We have interpolated the branching ratios for channels (1a)–(1d) to the assumed electron temperature at each altitude. To be consistent, we have also adopted their measured temperature-dependent rate coefficient of $2.75 \times 10^{-7}\,(300/T_e)^{0.55}\,cm^3\,s^{-1}$. The resulting velocity distributions for temperatures appropriate to the low and high solar activity exobases from previous models have been presented by *Fox and Haĉ* [1999], who found that 62–66% of the C atoms produced in dissociative recombination of CO^+ near the Martian exobase have enough energy to escape. Representative velocity distributions of C atoms from dissociative recombination of CO^+ at 190 km for the low solar activity model and at 230 km for the high solar activity model are shown in Figures 4a and 4b. The fractions of escaping ^{12}C (and ^{13}C) atoms are shown as a function of altitude from 170 to 300 km in Figure 5 along with their ratio. It can be seen that the fraction of ^{12}C that escapes is significantly larger than that of ^{13}C and is ~ 0.63 at 190 km and 0.61 at 220 km, near the low and high solar activity exobases, respectively. Since the variation of the escape fraction with altitude is not large, in order to estimate the escape fluxes we have multiplied the integrated dissociative recombina-

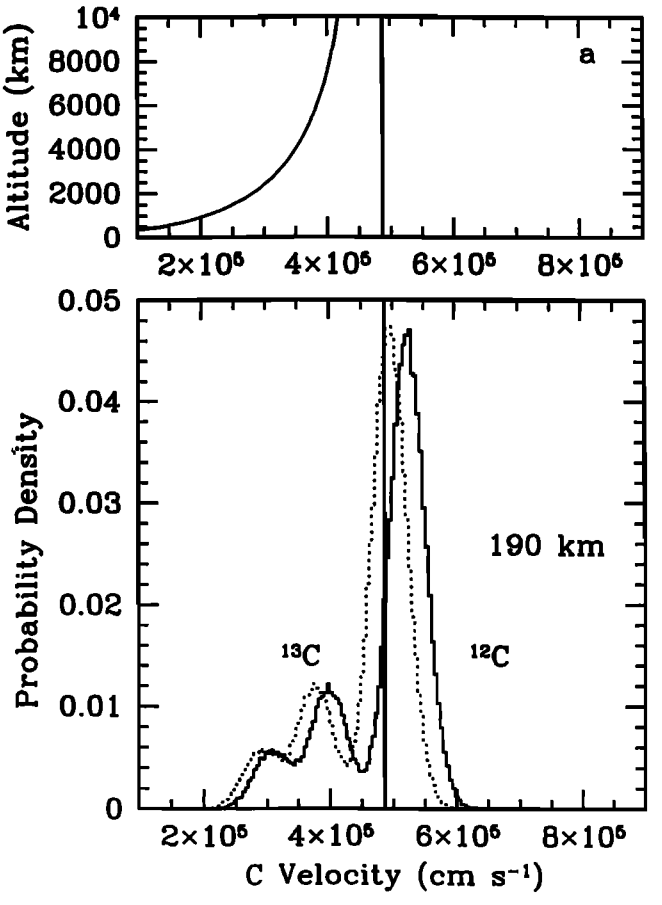

Figure 4. (a) (bottom) Velocity distribution of the C atoms produced in CO^+ dissociative recombination at 190 km (near the exobase) from a Monte Carlo calculation [cf. *Fox and Haĉ*, 1997]. (top) Altitude to which a C atom released vertically at that altitude with the velocity shown will rise if it does not undergo a collision. In both panels the vertical line is the escape velocity at 190 km on Mars. (b) Same as Figure 4a, but for the high solar activity model near 230 km.

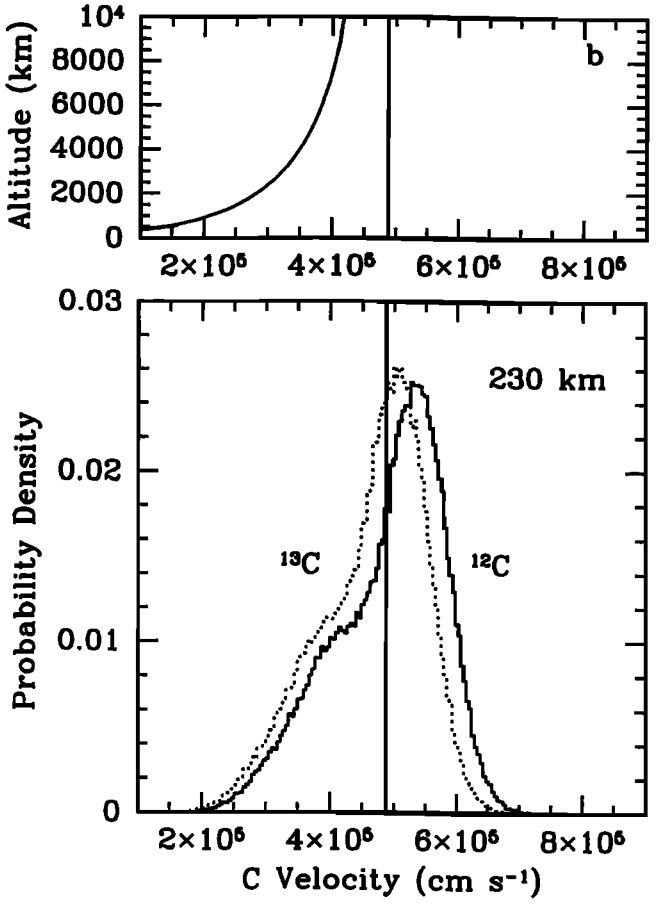

Figure 4. (continued)

tion rates above the exobases by the fractions near the exobases.

We have also computed the energy distribution of atomic carbon produced in photodissociation of CO as a function of altitude, with the assumption that both atoms are produced in the ground $C(^3P)$ and $O(^3P)$ states. *Cosby* [1993] found that for electrons with energies greater than ~30 eV, the ground state atoms dominated the products of electron impact dissociation, and it is likely that this is true for photodissociation also. In our calculations the energy range 0–6 eV is divided into 0.02 eV bins, and the probabilities of production of a C atom per energy bin for the low solar activity model at 180 and 200 km and for the high solar activity model at 210 and 230 km are shown in Figures 6a and 6b, respectively. While the peak of the distributions are in the range 1–1.5 eV, it is clear that many C atoms are released with energies in excess of the escape energy of ~1.48 eV. The computed fraction of C atoms with energies greater than the escape energy at 300 km is ~ 0.43 in the low solar activity model and ~ 0.45 in the high solar activity model; the fractions decrease monotonically to ~0.30 in both models at 170 km.

It is difficult to determine the fraction of C atoms produced with energies greater than the escape energy in electron impact dissociation of CO because the electron probably carries away a substantial amount of the energy. *Cosby* [1993] measured the center-of-mass energy released to the fragments in electron impact dissociation of CO and found that for energies greater than ~ 28.5 eV, near the peak of the cross section, the energy released ranges from 0.2 to 4.0 eV. For C to escape, the total energy released must be greater than 2.6 eV, and his measurements indicate that ~15% of the electron impact dissociations lead to fragments with total energies >2.6 eV. As mentioned previously, Cosby also determined that production of the ground states $C(^3P)$ + $O(^3P)$ was the dominant channel, but he did not rule out small branching ratios to channels producing atoms in excited states. Although the measured fragment energy distribution strictly applies to relatively high electron energies and to the energy released in the center-of-mass frame, we have adopted the value 0.15 for the fraction of C produced with the escape energy. The cross sections for electron impact dissociation are negligible below the threshold of 13.7 eV for production of C + O with total kinetic energies in excess of 2.6 eV. In fact, the appearance potential reported by Cosby was ~14 eV. The error introduced by this assumption is probably much less than the other uncertainties in this calculation.

We have assumed that photodissociative ionization of CO (reaction(4)) and photoelectron impact dissociative ionization (reaction(5)) lead to energetic atoms and ions. We have somewhat arbitrarily assumed that half the C atoms produced in both processes are released with energies greater than the escape energy. Although

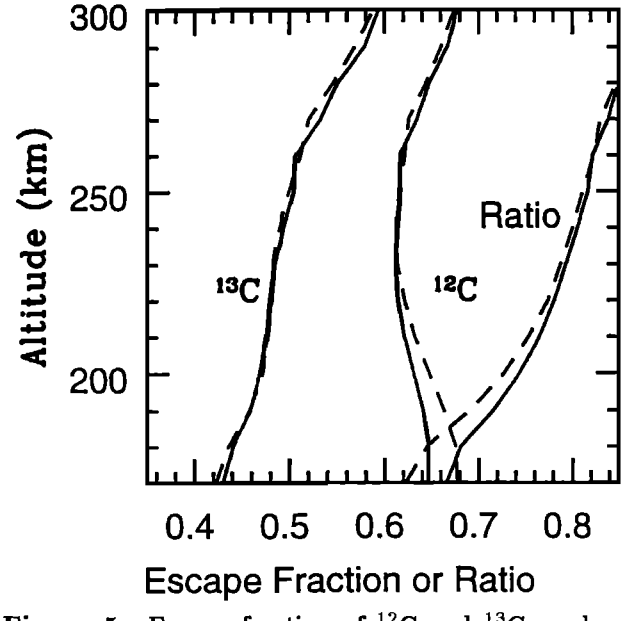

Figure 5. Escape fraction of ^{12}C and ^{13}C produced in dissociative recombination of CO^+ as a function of altitude along with their ratio from 170 to 300 km. The dashed curves are for low solar activity and the solid curves are for high solar activity.

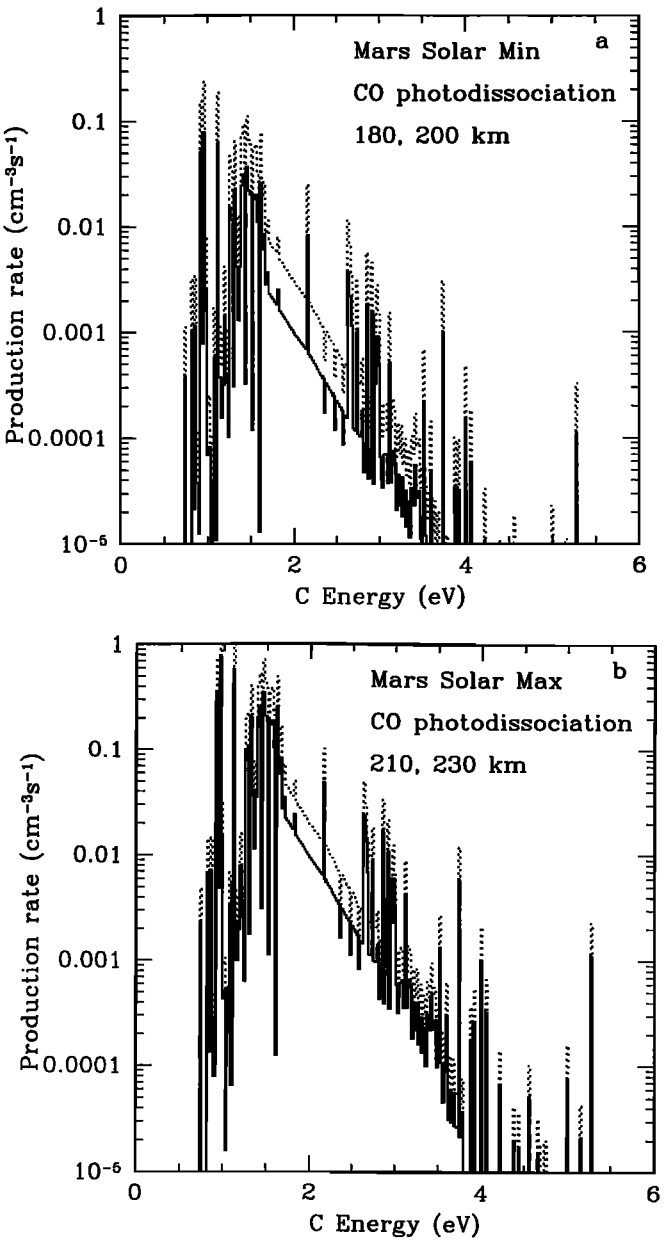

Figure 6. (a) Energy distribution of C atoms produced in photodissociation of CO at two altitudes for the low solar activity model. The ordinate is probability per 0.02 eV bin, normalized to the total photodissociation rate at each altitude. The dotted curve is for an altitude of 180 km, and the solid curve is for 200 km. (b) Same as Figure 6a, but for the high solar activity model. The dotted curve is for an altitude of 210 km, and the solid curve is for 230 km.

the rate coefficient for the dissociative charge transfer reaction of O^{++} with CO (reaction(6)) is unknown, we have assumed that it is the same as that for the reaction of O^{++} with N_2, $1.6 \times 10^{-9}\,cm^3 s^{-1}$, which is $\sim 80\%$ of gas kinetic [*Howorka et al.*, 1979], and that half the reactions produce neutral C and half produce C^+. Since we will show that with these assumptions, reactions (4), (5), and (6) are negligible as sources of escaping C, even large errors due to these assumptions would be unimportant for our calculations.

4. Results and Discussion

We have estimated the global average escape rates of processes (1)–(6) for the high solar activity model by integrating the rate of each process above the exobase, multiplying by the fraction of C atoms assumed to have energies greater than the escape energy, multiplying by half to account for the fraction released downward, and multiplying by half again to account for the lack of escape from the nightside. The results are shown in Table 1 for both low and high solar activity models and represent global average escape fluxes rather than hemispheric escape fluxes.

The most important escape mechanism is found to be photodissociation of CO, with a global average escape flux of 1.8×10^6 cm^{-2} s^{-1} at high solar activity. The low solar activity value is more than an order of magnitude smaller owing mostly to the combined effects of the smaller CO mixing ratio, smaller scale heights, and the reduced EUV fluxes. The escape flux of C from dissociative recombination of CO^+ is also highly sensitive to solar activity, increasing by a factor of >20 from 2.9×10^4 cm^{-2} s^{-1} to 6.2×10^5 cm^{-2} s^{-1} at high solar activity. The other four mechanisms contribute < 10% of the total escape flux for either model.

The calculated total global average escape flux of C from all photochemical processes at low solar activity is $\sim 2.1 \times 10^5$ cm^{-2} s^{-1}, whereas at high solar activity it is about $\sim 2.6 \times 10^6$ cm^{-2} s^{-1}. Since the solar activity dependence of the escape fluxes is not linear, we expect the time-averaged escape rates to be slightly smaller than the average of the low and high solar activity values.

We can compare our C escape fluxes with those computed by *Nagy et al.* [2001] using the two-stream method. Nagy et al. predicted global average escape fluxes of 2.7×10^5 and 3.9×10^6 cm^{-2} s^{-1} for low and high solar activities, respectively. These fluxes are 30–50% larger than our values. In addition to using slightly different cross sections, the models used here are somewhat different from those adopted by *Nagy et al.* [2001] and by *Fox and Haćic* [1999]. The previous high solar activity model was based on an earlier MTGCM model from S. Bougher (private communication, 1996). *Fox and Haćic* [1999] predicted escape fluxes due to dissociative recombination that were about 50% larger than the present values. In the previous high solar activity model we placed the exobase at 215 km, whereas in the present model it is near 220 km. Earlier versions of the low solar activity model (including that adopted by *Nagy et al.* [2001]) which were based on Viking 1 data, did not include H and H_2, which react with many ions, including CO^+, N_2^+, and CO_2^+. With the inclusion of these species the density profile of CO^+ and the escape flux of C due to dissociative recombination of CO^+ are both reduced. In fact, our low solar activity model O^+ peak

Table 1. Global Average C Photochemical Escape Fluxes

Process	Flux, $10^5\,cm^{-2}\,s^{-1}$	
	Low Solar Activity	High Solar Activity
$CO + h\nu \rightarrow C + O$	1.65	18
$CO^+ + e \rightarrow C + O$	0.29	6.2
$CO + h\nu \rightarrow C + O^+ + e$	0.090	1.0
$CO + e \rightarrow C + O + e$	0.065	0.77
$O^{++} + CO \rightarrow C + O^+ + O^+$	0.0027	0.023
$CO + e \rightarrow C + O^+ + 2e$	0.0011	0.012
Total	2.1	26

densities are a factor of 2 smaller than those measured by the Viking retarding potential analyzer [*Hanson et al.*, 1977] and the CO^+ densities are smaller than our previous models indicated by 25% at the peak and by a 60% at 300 km. Since the H and H_2 density profiles are anticorrelated with solar flux because of the increases in the escape rates and eddy diffusion coefficients from low to high solar activity [*Krasnopolsky et al.*, 1998], the effects of H and H_2 on the high solar activity ionosphere are not large. We do, however, feel that the H_2 mixing ratio of 40 ppm predicted by *Krasnopolsky et al.* [1998] is an overestimate. (It is also, of course, possible that the Viking 1 O^+ profile is in error or is not representative.) We will analyze more completely the effects of H_2 densities on the ionosphere of Mars in a future paper. Also, we will later include the chemistry of some of the products of reactions of ionospheric ions with H_2, such as N_2H^+, OH^+, HCO^+, and HCO_2^+. In the present calculations we have lost a small amount of mass and charge, which results in slight underestimates of the dissociative recombination rates. Since, however, the time-averaged escape rate is dominated by the high solar activity values, an uncertainty of the order of a factor of 2 in the low solar activity values is not significant.

The difference between our predictions for the escape flux due to photodissociation of CO and the values of *Nagy et al.* [2004] (a factor of slightly less than 1.5) may also be partly due to the use of the "exobase" approximation, in which only energetic atoms produced above the exobase are assumed to escape. Since the photodissociation rate increases as the altitude decreases, a large fraction of escaping atoms may arise from altitudes below the exobase. The CO^+ dissociative recombination rate also increases with decreasing altitude near the exobase, peaking in the 140–150 km range. We are in the process of carrying out Monte Carlo calculations to determine how reliable the exobase approximation is for estimating escape rates due to various mechanisms.

As mentioned previously, large fluxes of escaping ions attributed to O^+ were observed by instruments on the Phobos spacecraft [e.g., *Verigin et al.*, 1991; *Lundin et al.*, 1990], although there are large uncertainties in the total escape rates inferred from these measurements. Undoubtedly, some of the escaping ions contain carbon atoms. *Fox* [1997] placed an upper limit on the hemispheric escape fluxes of $CO_2^+ + CO^+ + C^+$ owing to the production rate above the photochemical equilibrium region of $4.2 \times 10^6\,cm^{-2}\,s^{-1}$ at low solar activity and $3.2 \times 10^7\,cm^{-2}$ at high solar activity. In the current low solar activity model, significant fractions of the CO_2^+ and CO^+ are destroyed in reactions with H_2. We have performed a similar computational experiment as that carried out by *Fox* [1997] and found that for the maximum upward velocity boundary condition on the ions ($\sim 7.9 \times 10^4\,cm\,s^{-1}$), which reproduces the Viking O_2^+ density profiles [*Hanson et al.*, 1977], the low solar activity upper limit on the hemispheric escape rate of C containing ions is $2.2 \times 10^6\,cm^{-2}\,s^{-1}$, which is smaller by about a factor of almost 2 than the earlier model indicates. As stated previously, we do not, however, consider the current low solar activity model to be more reliable than the Viking model, and furthermore, in the present model we do not include HCO^+ and HCO_2^+, the escape of which will also increase the C escape rates. The MHD calculations of *Liu et al.* [1999, 2001] predicted that the total ion escape fluxes were of the order of one fourth of the upper limits for $O_2^+ + O^+$ escape computed by *Fox* [1997]. If this factor is applied to the upper limits for the C-containing ion escape fluxes of *Fox* [1997], the global average C escape flux would be $(5\text{–}40) \times 10^5\,cm^{-2}\,s^{-1}$ where the range is from low to high solar activities. Clearly, ion escape has the potential to rival or even dominate photochemical escape. As pointed out previously, however, there are large uncertainties in both the computed and measured ion escape fluxes. Further research into ion escape mechanisms and spacecraft measurements of ion escape fluxes would be helpful.

The predicted photochemical escape fluxes are of the same order of magnitude as the global average escape flux from sputtering of $5 \times 10^5\ cm^{-2}\,s^{-1}$ for moderate solar activity as computed by *Kass* [1999] and $1 \times 10^5\,cm^{-2}\,s^{-1}$ for low solar activity as computed

Table 2. Comparison of Global Average C Escape Fluxes For Various Nonthermal Mechanisms

Process	Flux (10^5 cm^{-2} s^{-1})		
	Low Solar Activity	Moderate Solar Activity	High Solar Activity
Photochemical	2.1		26
Sputtering[a]		5	
Sputtering[b]	1		
Ion escape[c]	$\leq$ 21		$\leq$160

[a] From a moderate solar activity model [*Kass*, 1999].
[b] From a low solar activity model [*Luhmann et al.*, 1992; *Jakosky et al.*, 1994].
[c] From *Fox* [1997].

by *Luhmann et al.* [1992] (corrected by *Jakosky et al.* [1994]). The sputtering rates are, however, more uncertain than the photochemical escape rates at present. At earlier times the photochemical escape rates probably scaled as the solar EUV fluxes squared or cubed. This amplification is due to the combined effects of increases in the CO mixing ratios, the neutral temperatures, the ionization and dissociation rates, and the electron densities as the solar EUV fluxes increase. On the other hand, the sputtering rates are predicted to be larger by orders of magnitude at earlier epochs when the solar wind is predicted to be have been much more intense [*Zhang et al.*, 1993], although recent calculations by *Johnson and Luhmann* [1998] have shown that a feedback process in the sputtering contribution to the hot O corona may reduce the loss rates due to sputtering at earlier times. Although these calculations indicate that the photochemical escape rates are slightly more important at present, sputtering may have dominated the escape earlier in the history of the planet. The escape fluxes for various nonthermal mechanisms are compared in Table 2.

Finally, we address the effect on the escape rates of the small-scale magnetic crustal anomalies detected by the Mars Global Surveyor [e.g., *Acuña et al.*, 1999], which are found mostly in the ancient cratered terrain in the southern hemisphere. They indicate that Mars once had a magnetic dynamo but that it survived only a few hundred million years. Such a primordial field would considerably reduce the sputtering rates and would shelter the ionosphere from any direct interaction with the solar wind, allowing the ionopause to rise, possibly marginally increasing the escape rates due to dissociative recombination. The escape rate of C due to photodissociation of CO would not be affected by the presence of a magnetic field, although an increase in the solar EUV fluxes and the mixing ratio of CO at earlier epochs would certainly increase the photodissociation rate. The direct escape of ions would be shut off, except perhaps along open field lines in the polar regions.

At present, in regions above the remnant crustal fields the ionosphere may be magnetized, and its structure could be quite different from the structure assumed here, in which no magnetic field is assumed. The effects of localized magnetic anomalies on the ionosphere have been discussed by *Liu et al.* [2001], who predicted larger ion densities, and by *Ness et al.* [2000], who predicted smaller ion scale heights. Previously, *Shinagawa and Cravens* [1992] modeled the effect of an intrinsic magnetic field on Mars and suggested that even for the case in which the intrinsic magnetic field was smaller than that induced by the solar wind interaction, the ion densities at high altitudes would be reduced by a strong horizontal plasma flow. This would lead to a significant decrease in the ion densities with increasing altitudes and thus to smaller ion and electron density scale heights, also. Further model calculations and measurements of the structure of the ionosphere in the regions of the magnetic anomalies are essential to determining definitively the effect of the magnetic field on the ion density profiles and the escape rates.

5. Summary and Conclusions

We have computed the photochemical escape rates of atomic carbon for low and high solar activity models due to six sources: photodissociation of CO, dissociative recombination of CO^+, electron impact dissociation of CO, photodissociative ionization and electron impact dissociative ionization of CO, and the dissociative charge transfer reaction of O^{++} with CO. The global average escape fluxes for each source and totals at low and high solar activities are given in Table 1. The largest sources are photodissociation of CO and dissociative recombination of CO^+, while the other sources contribute $< 10\%$ of the total. The escape fluxes increase by factors of 10–20 from low to high solar activities, and the escape flux due to dissociative recombination shows the largest variation with solar activity. The total global average escape fluxes are 2.1×10^5 and 2.6×10^6 cm^{-2} s^{-1} at low and high solar activities, respectively. The time-

averaged escape rate of C will be controlled mostly by the high solar activity values, and an average photochemical escape flux of $\sim 1 \times 10^6$ cm^{-2} s^{-1} is predicted.

The C escape fluxes from photochemical sources are slightly larger than current estimates for the escape flux due to sputtering at present [e.g., *Kass*, 1999; *Luhmann et al.*, 1992; *Jakosky et al.*, 1994]. In previous epochs, when the solar fluxes were predicted to have been enhanced by factors of 3–6 at 2.5–3.5 Gyr before present, the photochemical escape rates probably scaled as the solar flux squared or cubed, whereas the sputtering fluxes are predicted to have increased by orders of magnitude [*Zhang et al.*, 1993; *Johnson and Luhmann*, 1998]. Although the sputtering rates are highly uncertain even at present, sputtering may have dominated the escape of C in the past.

Acknowledgments. This work has been supported in part by NASA grant NAG5-6879 and by NSF grant AST-9802007 to the Research Foundation of the State University of New York at Stony Brook.

Janet G. Luhmann thanks Robert E. Johnson and another referee for their assistance is evaluating this paper.

References

Acuña, M. H., et al., Global Distribution of Crustal Magnetization Discovered by the Mars Global Surveyor MAG/ER Experiment, *Science, 284*, 790–793, 1999.

Anderson, D. E., and C. W. Hord, Mariner 6 and 7 ultraviolet spectrometer experiment: Analysis of hydrogen Lyman-alpha data, *J. Geophys. Res., 76*, 6666, 1971.

Ayres, T., Evolution of the solar ionizing flux, *J. Geophys. Res, 102*, 1641, 1997.

Bailey, S. M., T. N. Woods, C. A. Barth, S. C. Solomon, L. R. Canfield, and R. Korde, Measurements of the solar soft X-ray irradiance by the Student Nitric Oxide Explorer: First analysis and underflight calibrations, *J. Geophys. Res., 105*, 27,179, 2000.

Barth, C. A., C. W. Hord, J. B. Pearce, K. K. Kelly, G. P. Anderson, and A. I. Stewart, Mariner 6 and 7 ultraviolet spectrometer experiment: Upper atmospheric data, *J. Geophys. Res., 76*, 2213, 1971.

Balakrishnan, N., V. Kharchenko, and A. Dalgarno, Quantum mechanical and semiclassical studies of N + N_2 collisions and their applications to thermalization of fast N atoms, *J. Chem. Phys., 108*, 943–949, 1998.

Bougher, S. W., R. G. Roble, E. C. Ridley, and R. E. Dickinson, The Mars thermosphere, 2, General circulation with coupled dynamics and composition, *J. Geophys. Res., 95*, 14,811, 1990.

Chen, R. H., T. E. Cravens, and A. F. Nagy, The Martian ionosphere in light of the Viking observations, *J. Geophys. Res., 83*, 3871, 1978.

Cosby, P. C., Electron-impact dissociation of carbon monoxide, *J. Chem. Phys., 98*, 7804–7818, 1993.

Fox, J. L., Atomic carbon in the atmosphere of Venus, *J. Geophys. Res., 87*, 9211, 1982. (Correction, *J. Geophys. Res., 90*, 11,106, 1985.)

Fox, J. L., On the escape of oxygen and hydrogen from Mars, *Geophys. Res. Lett., 20*, 1747, 1993.

Fox, J. L., Upper limits to the outflow of ions at Mars: Implications for atmospheric evolution, *Geophys. Res. Lett., 24*, 2901, 1997.

Fox, J. L., Photochemical escape of C from Mars, *Bull. Am. Astron. Soc., 31*, 5905, 1999.

Fox, J. L. Spectrum of atomic carbon produced in photodissociation of CO on Mars: Implications for atmospheric evolution, *Bull. Am. Astron. Soc., 32*, 5124, 2000.

Fox, J. L., and J. H. Black, Photodissociation of CO in the thermosphere of Venus, *Geophys. Res. Lett. 16*, 291, 1989.

Fox, J. L., and A. Hać, Velocity distributions of C atoms in CO^+ dissociative recombination: Implications for atmospheric evolution, *J. Geophys. Res., 104*, 24,729, 1999.

Fox, J. L. and K. Sung, Solar activity variations in the Venus ionosphere/thermosphere, *J. Geophys. Res., 106*, 21,305, 2001.

Fox, J. L., P. Zhou, and S. W. Bougher, The thermosphere/-ionosphere of Mars at high and low solar activities, *Adv. Space Res., 17* (11), 203–218, 1995.

Geoghegan, M., N. G. Adams, and D. Smith, Determination of the electron-ion dissociative recombination coefficient for several molecular-ions at 300 K, *J. Phys. B. At. Mol. Opt. Phys., 24*, 2589–2599, 1991.

Hanson, W. B., S. Sanatani, and D. R. Zuccaro, The Martian ionosphere as observed by the Viking retarding potential analyzers, *J. Geophys. Res., 82*, 4351, 1977.

Hodges, R. R., Distributions of hot oxygen for Venus and Mars, *J. Geophys. Res., 105*, 6971, 2000.

Howorka, F., A. A. Viggiano, D. L. Albritton, E. E. Ferguson, and F. C. Fehsenfeld, Laboratory studies of O^{++} reactions of ionospheric importance, *J. Geophys. Res., 84*, 5941, 1979.

Jakosky, B. M., Mars volatile evolution: Evidence from stable isotopes, *Icarus, 94*, 14–31, 1991.

Jakosky, B. M., and J. H. Jones, The history of Martian volatiles, *Rev. Geophys., 35*, 1–16, 1997.

Jakosky, B. M., R. O. Pepin, R. E Johnson, and J. L. Fox, Mars atmospheric loss and isotopic fractionation by solar-wind-induced sputtering and photochemical escape, *Icarus, 111*, 271–288, 1994.

Johnson, R. E., and M. Liu, The loss of atmosphere from Mars, *Science, 274*, 1932, 1996.

Johnson, R. E., and J. G. Luhmann, Sputter contribution to the atmospheric conona on Mars, *J. Geophys. Res., 103*, 3649, 1998.

Johnson, R. E., D. Schnellenberger, and M. C. Wong, The sputtering of an oxygen thermosphere by energetic O^+, *J. Geophys. Res., 105*, 1659, 2000.

Kass, D. M., Change in the Martian atmosphere, Ph.D. Thesis, Calif. Inst. of Technol., Pasadena, Calif., 1999.

Kass, D. M., and Y. L. Yung, Loss of atmosphere from Mars due to solar wind sputtering, *Science, 268*, 697, 1995.

Kass, D. M., and Y. L. Yung, Response: The loss of atmosphere from Mars, *Science, 274*, 1932, 1996.

Kharchenko, V., J. Tharamel, and A. Dalgarno, Kinetics of thermalization of fast nitrogen atoms beyond the hard sphere approximation, *J. Atmos. Sol. Terr. Phys., 59*, 107–115, 1997.

Kharchenko, V., A. Dalgarno, B. Zygelman, and J.-H. Yee, Energy transfer in collisions of oxygen atoms in the terrestrial atmosphere, *J. Geophys. Res., 105*, 24,899, 2000.

Kim, J., A. F. Nagy, J. L. Fox, and T. E. Cravens, Solar cycle variation of hot oxygen atoms in the Martian upper atmosphere, *J. Geophys. Res, 103*, 29,339, 1998.

Krasnopolsky, V. A., Atomic carbon in the atmospheres of Venus and Mars, *Cosmic Res., Engl. Transl., 20*, 530, 1982.

Krasnopolsky, V. A., Solar cycle variations of the hydrogen escape rate and the CO mixing ratio on Mars, *Icarus, 101*, 33–41, 1993a.

Krasnopolsky, V. A., Photochemistry of the Martian atmosphere (mean conditions), *Icarus, 101*, 313–332, 1993b.

Krasnopolsky, V. A., On the deuterium abundance on Mars and some related problems, *Icarus, 148*, 597–602, 2000.

Krasnopolsky, V. A., and G. R. Gladstone, Helium on Mars: EUVE and PHOBOS data and implication for Mars' evolution, *J. Geophys. Res., 101*, 15,765, 1996.

Krasnopolsky, V. A., M. J. Mumma, and G. R. Gladstone, Detection of Atomic Deuterium in the Upper Atmosphere of Mars, *Science, 280*, 1576, 1998.

Lammer, H., and S. J. Bauer, Nonthermal atmospheric escape from Mars and Titan, *J. Geophys. Res., 96*, 1819, 1991.

Lammer, H., W. Stumptner, and S. J. Bauer, Loss of H and O from Mars: Implications for the planetary loss of water, *Geophys. Res. Lett., 23*, 3353, 1996.

Laubé, S., L. Lehfaoui, B. R. Rowe, and J. B. A. Mitchell, The dissociative recombination of CO^+, *J. Phys. B. At. Mol. Phys., 31*, 4181–4189, 1998.

Liu, Y., A. F. Nagy, C. P. T. Groth, D. L. DeZeeuw, T. I. Gombosi, and K. G. Powell, 3D Multi-fluid MHD studies of the solar wind interaction with Mars, *Geophys. Res. Lett., 26*, 2689, 1999.

Liu, Y., A. F Nagy, T. I. Gombosi, D. L. DeZeeuw, and K. G. Powell, The solar wind interaction with Mars: Results of three-dimensional three species MHD studies, *Adv. Space Res.*, (in press), 2001.

Luhmann, J. G., Correction to "The ancient oxygen exosphere of Mars: Implications for atmospheric evolution", *J. Geophys. Res., 102*, 1637, 1997.

Luhmann, J. G., R. E. Johnson, and M. H. G. Zhang, Evolutionary impact of sputtering of the Martian atmosphere by O^+ pickup ions, *Geophys. Res. Lett., 19*, 2151, 1992.

Lundin, R., A., et al., ASPERA/Phobos measurements of the ion outflow from the Martian ionosphere, *Geophys. Res. Lett., 17*, 873, 1990.

Mathur, D., and J. H. D. Eland, Dissociative ionisation of CO by 22.5–48.5 eV photons: Kinetic energy measurements of fragment ions by coincidence time-of-flight mass spectrometry, *Int. J. Mass. Spectrom. Ion Proc., 114*, 1123–136, 1992.

McElroy, M. B., Mars: An evolving atmosphere, *Science, 175*, 443, 1972.

McElroy, M. B., T. Y. Kong, and Y. L. Yung, Photochemistry and evolution of Mars' atmosphere: A Viking perspective, *J. Geophys. Res., 82*, 4379, 1977.

Mentzoni, M. H., and J. Donohoe, Electron recombination and diffusion in CO at elevated temperatures, *Can. J. Phys., 47*, 1789, 1969.

Mitchell, J. B. A., The dissociative recombination of molecular ions, *Phys. Rep., 186*, 215, 1990.

Mitchell, J. B. A. and H. Hus, The dissociative recombination and excitation of CO^+, *J. Phys. B. At. Mol. Phys., 18*, 547–555, 1985.

Morgan, H. D., and J. E. Mentall, EUV studies of N_2 and O_2 produced by low energy electron impact, *J. Chem. Phys., 78*, 1747–1757, 1983.

Nagy, A., M. Liemohn, J. L. Fox, and J. Kim, Hot carbon densities in the exosphere of Mars, *J. Geophys. Res., 106*, 21,565, 2001.

Nair, H., M. Allen, A. D. Anbar, Y. L. Yung, and R. T. Clancy, A photochemical model of the Martian atmosphere, *Icarus, 111*, 124–150, 1994.

Ness, N. F., M. H. Acuña, J. E. P. Connerney, A. J. Kliore, T. K. Breus, A. M. Krymskii, P. Cloutier, and S. J. Bauer, Effects of magnetic anomalies discovered at Mars on the structure of the Martian ionosphere and solar wind interaction as follows from radio occultation experiments, *J. Geophys. Res., 105*, 15,991, 2000.

Nier, A. O., and M. B. McElroy, Structure of the neutral upper atmosphere of Mars: Results from Viking 1 and Viking 2, *Science, 194*, 1298, 1976.

Nier, A. O., and M. B. McElroy, Composition and structure of Mars' upper atmosphere: Results from the neutral mass spectrometers on Viking 1 and 2, *J. Geophys. Res., 82*, 4341, 1977.

Paxton, L. J., Atomic carbon in the Venus thermosphere: Observations and theory, Ph.D. thesis, Univ. of Colorado, Boulder, Colo., 1983.

Rohrbaugh, R. P., J. S. Nisbet, E. Bleuler, and J. R. Herman, The effect of energetically produced O_2^+ on the ion temperatures of the Martian thermosphere, *J. Geophys. Res., 84*, 3327, 1979.

Rosén, S., R. Peverall, M. Larsson, A. Le Padellec, J. Semaniak, Å Larson, C. Strömholm, W. J. van der Zande, H. Danared, and G. H. Dunn, Absolute cross sections and final state distributions for dissociative recombination and excitation of $CO^+(v = 0)$ using an ion storage ring, *Phys. Rev. A, 57*, 4462–4471, 1998.

Samson, J. A. R., and J. L. Gardner, Partial photoionization cross sections and branching ratios of CO from 750 to 304 Å, *J. Electron Spectrosc. Relat. Phenom., 8*, 35, 1976.

Shinagawa, H., and T. E. Cravens, The ionospheric effects of a weak intrinsic magnetic field at Mars, *J. Geophys. Res., 97*, 1027, 1992.

Sung, K., and J. L. Fox, Electron impact cross sections for use in modeling the ionospheres/thermospheres of the earth and planets, *Eos Trans. Am. Geophys. Union, 81*(48), Fall Meet. Supple., SA52A-11, 2000.

Tobiska, W. K., Revised solar extreme ultraviolet flux model, *J. Atmos. Terr. Phys., 53*, 1005, 1991.

Torr, M. R., D. G. Torr, R. A. Ong, and H. E. Hinteregger, Ionization frequencies for major thermospheric constituents as a function of solar cycle 21, *Geophys. Res. Lett., 6*, 771, 1979.

Tully, C., and R. E. Johnson, Low energy collisions between ground state oxygen atoms, *Planet. Space Sci., 49*, 533–537, 2001.

Verigin, M. I., et al., Ions of planetary origin in the Martian magnetosphere (PHOBOS 2/TAUS experiment), *Planet. Space Sci., 39*, 131–137, 1991.

Wallis, M. K., C, N, and O isotope fractionation on Mars: Implications for crustal H_2O and SNC meteorites, *Earth Planet. Sci. Lett., 93*, 321–324, 1989.

Zhang, M. H. G., J. G. Luhmann, S. W. Bougher, and A. F. Nagy, The ancient oxygen exosphere of Mars: Implications for atmospheric evolution, *J. Geophys. Res., 98*, 10,915, 1993.

F. M. Bakalian, Marine Sciences Research Center, State University of New York at Stony Brook, Stony Brook, NY 11794-5000, USA. (faez@platmo.phy.wright.edu)

J. L. Fox, Department of Physics, Wright State University, Dayton, OH 45435, USA. (fox@platmo.phy.wright.edu)

(Received April 13, 2001; revised June 21, 2001; accepted June 25, 2001.)